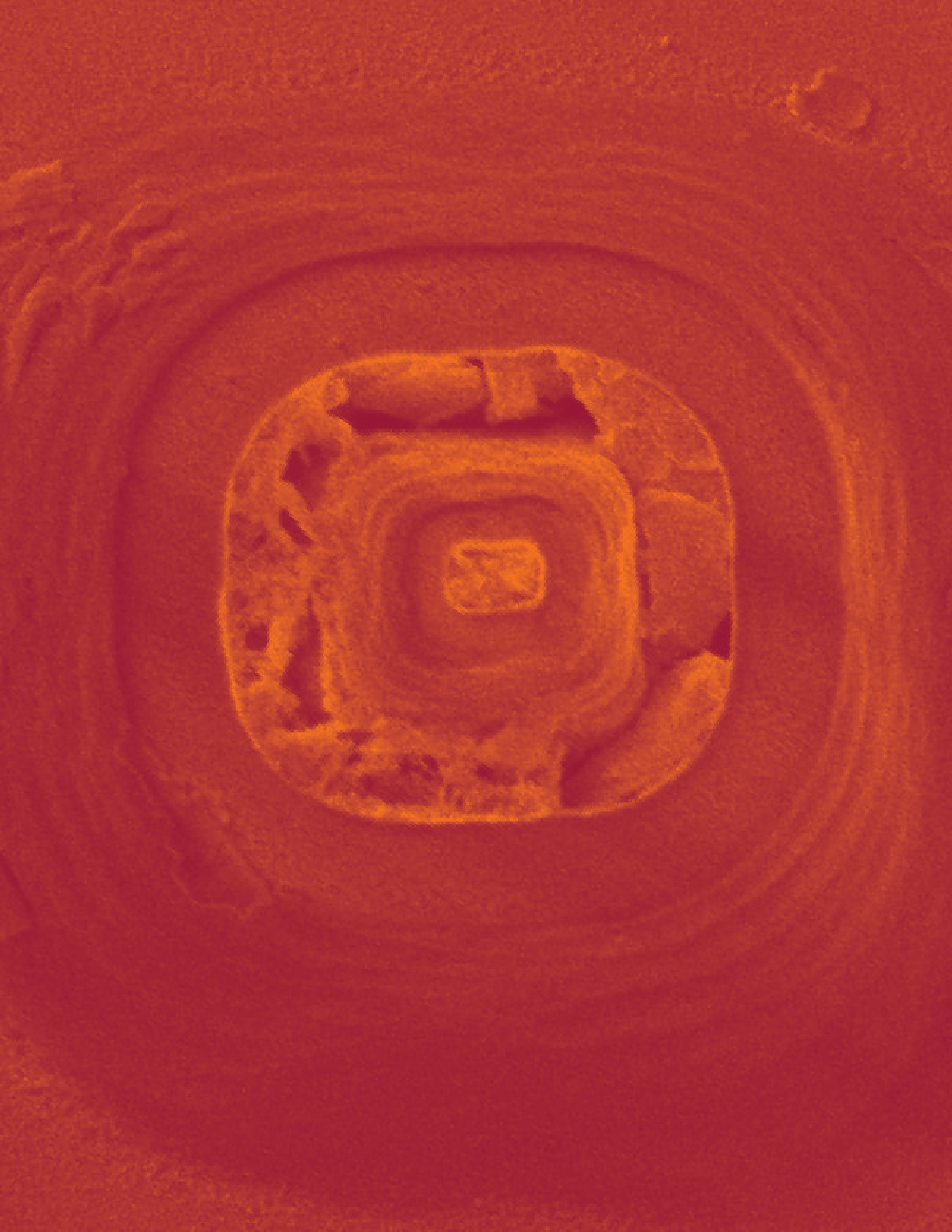

Sol-Gel Ink Patterning Using Fountain-Pen Nanolithography

Undergraduate Researcher
Eduardo Aramayo
Illinois Institute of Technology

Faculty Mentor
Horacio D. Espinosa
Department of Mechanical Engineering
Northwestern University

Graduate Student Mentor
Andrea Ho
Department of Mechanical Engineering
Northwestern University

Abstract

This research investigated the feasibility of patterning with sol-gels using a nanofountain probe in an atomic force microscope. Two oxide sols — barium titanate and cobalt ferrite — were used as inks in patterning tests using fountain-pen nanolithography (FPN). This was shown to be a suitable method of depositing sol-gels on silicon, silicon nitride, and gold substrates. One area of further study might involve the effects of environmental conditions such as relative humidity on sol-gel ink patterning using FPN.

Introduction

The ability to deposit nanoscale materials on a surface in an orderly arrangement is essential in nanomanufacturing, and several patterning techniques have been developed over the years. For example, nanoimprint lithography is a stamp method that creates patterns by the mechanical deformation of imprint resist. Photolithography is an etching process that uses a photomask and light-sensitive chemicals, and soft lithography uses elastomeric stamps, molds, and photomasks.[1] These and other contact printing and stamp methods are relatively simple techniques. But they have some drawbacks and limitations: they tend to lack resolution, especially when compared to scanning probe lithographic and electron beam methods; they function poorly when printing with multiple inks; and they all involve complicated fabrication processes and equipment. The challenge is to develop a low-cost technique that offers high resolution.[2,3]

Direct-write patterning methods are becoming increasingly popular because of their relative simplicity and low cost. One of the latest direct-write methods is fountain-pen nanolithography (FPN), a novel technique still being explored and modified to improve functionality. A key part of this investigation is determining how well FPNs can write with different inks and how external changes (temperature, scan speeds, etc.) affect this ability.

Background

A patterning method known as dip-pen nanolithography (DPN) was developed in 1999 by Chad A. Mirkin and colleagues at Northwestern University. This direct-write soft lithography technique uses a conventional atomic force microscope (AFM) with a contact tip. An AFM provides topographical and friction maps of surfaces by raster-scanning a surface with a fine tip mounted on a cantilever. A laser beam reflects off the end of the cantilever onto a photodetector. Recording tip movements creates a "map" of the surface. When the tip is in contact with the surface, the small gap between the two condenses water on the substrate surface. DPN uses this natural water condensation, called a water meniscus, to transport molecules from the tip to the substrate.[5] The molecules, or "ink", diffuse via capillary transport and anchor themselves on the substrate through chemisorption or electrostatic interactions.[2,3,5]

DPN is coming into wider use as the technology advances (current resolution is on the sub-100 nm scale). A large part of its appeal lies in its use of conventional atomic force microscopy instead of processing methods that require special equipment. However, DPN has limitations. The conventional probe it uses for reading and writing on a surface needs regular molecular ink replenishment.[6,7] This requires periodic realignment of the probe tip during patterning, which limits throughput. The need for diffusion time also limits writing speeds.

Fountain pen nanolithography (FPN) addresses some of these shortcomings. With FPN, a microfluidic chip is mounted in an AFM with a reservoir to deliver liquid materials to a surface through an annular aperture. The aperture is located at the apex of a hollow pyramidal tip that resembles a volcano (Figure 1a).[6,8] The annular aperture controls the position of the liquid-air interface at the aperture. The basic FPN structure allows ink to feed into the reser-

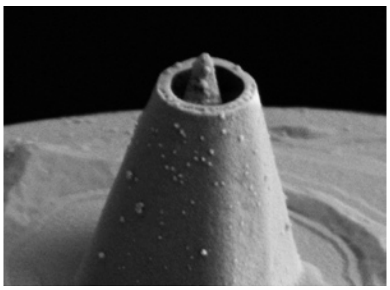

A

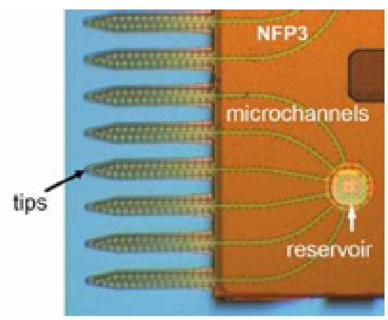

B

Figure 1. (a) SEM image of the volcano tip of a nanofountain probe. (b) Optical image of a front-side view of a nanofountain probe.[10]

voir on top of the chip. Then capillary action drives the ink through a microchannel down the cantilever to the "volcano tip" to form the liquid-air interface around the tip. Having this interface close to the tip contributes to the capillary condensation meniscus, which helps the probe flow ink onto the substrate.[6–9]

A diagram of the FPN patterning process is shown in Figure 2. Third-generation chips, as seen in Figure 1b, have larger reservoirs that hold more ink, and are fabricated on SOI (silicon-on-insulator) wafers. They also have deeper, better-sealed microchannels to improve flow. Chips contain four reservoirs connecting to six tips each (24 tips total), allowing 12 tips to operate simultaneously in parallel.[10] Furthermore, complex patterning involving multiple inks is possible with a single chip because each reservoir on a probe can hold a different ink without cross-contamination. The same reservoir can be used for multiple ink feeds of the same solution within a single day without requiring cleaning.[6–9]

Both DPN and FPN resolutions depend on temperature, water condensation layer size, ink-substrate chemical interaction, scan speeds, number of traces, contact time, and fineness of the tip.[2,7–8,11–12] Applying a voltage also changes resolution. Choices of ink and substrate are also key factors in resolution because surface features of the substrate affect interaction with the ink.

Similar to DPN, FPN can be used for both reading and writing. The FPN functions well when imaging its own patterns via friction measurements, but, like DPN, it risks contaminating unpatterned regions. The FPN writing process produces results with as much consistency as DPN; an FPN chip, however, can hold more ink than a conventional contact mode tip. This means FPN patterning can create more patterns in a single pass.

Many aspects of FPN are open to further investigation, including how well it performs with different inks. Here, a fluorescent dye (dextran) in deionized water was used to prove the chip's functionality. Solutions of ODT (1-octodecanethiol) and MHA (16-mercaptohexadecanoic acid) were used to test functionality on a gold substrate. PFT (1H, 1H, 2H, 2H-Perfluorododecane-1-thiol), FITC-labeled DNA, and gold nanoparticles were also tested and shown to be functional in FPN chips.[8,10]

Sol-gels make up some of the toughest ceramics and lightest materials. The sol-gel process can be used to make

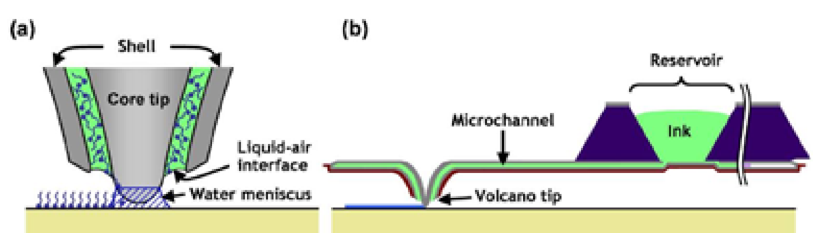

Figure 2. Diagram of how fountain-pen nanolithography works.[6]

ceramics, glasses, thin films, lenses, mirrors, membranes, aerogels, and xerogels. The most common printing technique using sol-gels is inkjet printing, but spraying, spin-coating, and dip-coating methods are also widely used. None of these methods offers the reliability or repeatability of FPN. Barium ferrite ($BaFe_{12}O_{19}$, or BaFe), aluminum oxide (Al_2O_3), silicon oxide (SiO_2), and tin oxide (SnO_2) have been successfully patterned on silicon and silicon oxide substrates using DPN.[13–14] Using sol-gels with FPN could prove useful in making optics, electronics, biosensors, and filtration systems.

Two oxide sols — the acetic acid–based ferroelectric compound barium titanate ($BaTiO_3$) and the nitric acid–based ferromagnetic compound cobalt ferrite ($CoFe_2O_4$) — are commonly used in patterning.[15–16] Cobalt ferrite is used with lead zirconium titanate in the fabrication of radially stacked hetero-structures (Figure 3) because of its high magnetostrictivity. These multifunc-tional oxide heterostructures can be used for microelectromechanics, optoelectron-ics, microwave devices, and data storage. Soft electron-beam lithography (eBL) allows for oxide heterostructure fabrication without feature alignment or etching, but the technique is expensive.[17] The goal of this research was to explore the compatibility of sol-gels with the FPN method.

Approach

To remove the residual organics, silicon substrates were cleaned in piranha solution (7:3 H_2SO_4:H_2O_2 by volume) at 90° C for 5 min, then sonicated in deionized water, and finally rinsed in ethanol and deionized water. Reference marks were made to indicate location during writing tests.

Droplets of deionized water and each sol, 0.10 µl each, were placed on cleaned glass, gold, silicon, cleaned silicon, silicon nitride, and gold substrates to examine the droplets' contact angles with a contact angle meter (VCA Optima contact angle measurement system). This was to confirm that the sol-gels would wet the substrate.

A 0.15 µl droplet of barium titanate ($BaTiO_3$) was placed in the chip reservoirs using a micropipette. The FPN was then mounted and configured in a conventional AFM (Veeco Dimension 3100). The AFM was set to operate in contact mode under constant-force mode. Each FPN chip underwent a series of writing experiments on both silicon and silicon nitride. The first test was a 25-dot test in which the tip was held in the same location five times for 2 sec each time, then again for 4, 8, 16, and 32 sec with a scan speed of 20 µm/s during the writing process. The next test involved drawing a 10 µm square at writing speeds ranging from 0.1 µm/s up to 200 µm/s. The final test created two dots 4 µm apart, with writing times of 8 and 32 sec. Using a different FPN chip, 0.15 µl of cobalt ferrite ($CoFe_2O_4$) went through the same process and writing tests. A third sol, a modified cobalt ferrite solution containing glycerol (5:1 cobalt ferrite: glycerol by volume) labeled with Rhodamine 6G, was also used to examine patterning of a more viscous solution of the sol. All imaging processes were scanned in tapping mode at 30 µm/s using the same AFM to create a map of the surface. Patterning conditions were held at 24–26° C and 55–65% relative humidity.

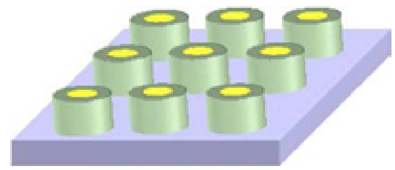

A

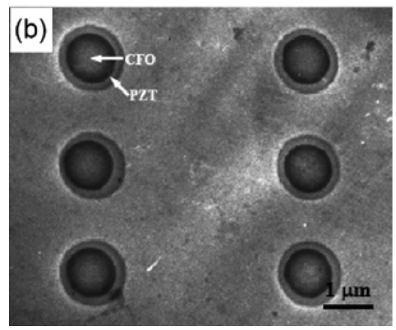

B

Figure 3. (a) Schematic of the columnar core and shell structure of radially stacked multifunc-tional oxide heterostructures. (b) TEM image of lead zirconium titanate (PZT) shell and cobalt ferrite (CFO) core heterostructures on an amorphous silicon nitride membrane.[17]

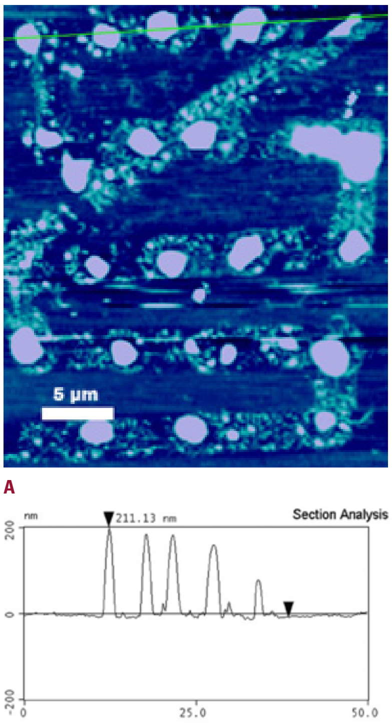

A

B

Figure 4. (a) Tapping-mode AFM image of a 5 x 5 cobalt ferrite dot array on a silicon substrate. Five rows of five dots each were created, with writing times of 2, 4, 8, 16, and 32 sec. (b) Section view along the line in (a) A section elevation (across the white line in [a]) shows the dots are 211 nm high.

Results and Discussion

Contact Angles

The measured contact angles were very low. Barium titanate had lower contact angles on all substrates, which demonstrated its extremely hydrophilic nature. The tests also showed that the modified cobalt ferrite solution was less hydrophilic than the pure sol. Contact angles decreased on substrates in the following order: gold (the most hydrophobic substrate), silicon nitride, glass, silicon with an oxide layer, and bare silicon treated with piranha solution (the most hydrophilic). These contact angles suggest that the inks would wet the substrates sufficiently to be transferred from the FPN tip to the substrate.

Cobalt Ferrite Sols

The sols were highly hydrophilic and tended to flow readily during patterning as well as scanning. To avoid smearing, the patterns were heated to 130° C after patterning for 5 min to solidify the patterns. Then they were scanned in tapping mode and imaged with an SEM. The silicon nitride FPN chip was at times modified with a gold film on its reservoir side to enhance the AFM laser signal sent to the photodetector. Only FPNs without this gold layer produced patterns. The cobalt ferrite proved to be a suitable ink for FPN patterning on both silicon and silicon nitride substrates, producing several patterns (Figure 4). The patterns were accurate except where the FPN tip was dragged across the pattern, depositing more cobalt ferrite. The dot-array layout was not as perfectly aligned as the code, because the AFM lacks a closed-loop feedback system in the x- and y-directions. The modified cobalt ferrite sol also patterned successfully on all three substrates and yielded similar results.

Barium Titanate

The barium titanate failed to produce any patterns on silicon, bare silicon, silicon nitride, and gold substrates. The sol flowed through the FPN to the tip, confirmed by an SEM image of the tip containing ink (Figure 5). The reason for the inability to pattern barium titanate using the FPN method is unknown and requires further investigation. A possible explanation might be unsuitable surface chemistry for the barium titanate to anchor to the substrates. Another theory is the sol is too hydrophilic and has contact angles too low to wet the substrate. A more viscous solution of barium titanate might increase the contact angle and create a more hydrophobic sol that might be able to be used for FPN patterning. Viscosity could be increased by introducing additives such as glycerol or increasing the sol's concentration.

Future Work

Further investigations will examine the viability of a host of sol-gels and FPN in hopes of furthering these methods. Explorations of ink modifications and possible improvements to the FPN tip might lead to better resolution and improved patterning. The influence of environmental factors on FPN patterning, specifically how relative humidity affects resolution, is still not entirely understood. FPN fabrication methods could be improved to lower costs and improve the likelihood of producing functioning chips.

Conclusion

FPN patterning of cobalt ferrite on silicon and silicon nitride substrates proved an effective approach for writing in nanofabrication. The sol's hydrophilic tendencies were important in the patterning process because they did not allow the patterns to be read using FPNs without heating. Barium titanate patterning, however, was not possible with FPN. Future work will explore the feasibility of FPN with a variety of sol-gels on different substrates.

This research was supported primarily by the Nanoscale Science and Engineering Initiative of the National Science Foundation under NSF Award Number ***EEC-0647560.*** *Any opinions, findings and conclusions or recommendations expressed in this material are those of the author(s) and do not necessarily reflect those of the National Science Foundation.*

References

(1) Rogers, D. Nanolithography. In *Nanostructures — Fabrication and Analysis;* Nejo, H., Ed. Springer-Verlag: Berlin, 2007.

(2) Piner, R. D.; Zhu, J.; Xu, F.; Hong, S.; Mirkin, C. A. *Science* **1999,** *283,* 661–663.

(3) Hong, S.; Zhu, J.; Mirkin, C. A. *Science* **1999,** *286,* 523–525.

(4) NT-MDT. "SPM Techniques/ Principles: AFM," *www.ntmdt.ru.*

(5) Mirkin, C. A.; et al, Mirkin group, DPN subgroup. *chemgroups. northwestern.edu/mirkingroup.*

(6) Kim, K. H.; Moldovan, N.; Espinosa, H. D. *Small* **2005**, *6,* 632–635.

(7) Moldovan, N.; Kim, K. H.; Espinosa, H. D. *J. Microelec. Sys.* **2006,** *15.1,* 204–213.

(8) Moldovan, N.; Kim, K. H.; Espinosa, H. D. *J. Micromech. Microeng.* **2006,** *16,* 1935–1942.

(9) Kim, K. H.; Moldovan, N.; Ke, C.; Espinosa H. D. *Mat. Res. Soc. Symp. Proc.* **2004,** *782.* Fall MRS Meeting, A5.56.1

(10) Wu, B.; Ho, A.; Moldovan, N.; Espinosa, H. D. *Langmuir* **2007,** *23,* 9120.

(11) Rozhok, S.; Piner, R.; Mirkin, C. A. *J. Phys. Chem. B* **2003,** *107,* 751–757.

(12) Nocedal, I.; Espinosa, H. D. ; Kim, K. H. *Nanoscape* **2005,** *2.1,* 105–111.

(13) Fu, L.; Liu, X.; Zhang, Y.; Dravid, V.P.; Mirkin, C. A. *Nano Lett.* **2003**, *3.6*, 757–760.

(14) Su, M.; Liu, X.; Li, S. Y.; Dravid, V. P.; Mirkin, C. A. *J. Am. Chem. Soc.* **2002,** *124.8,* 1560–1561.

(15) Chinnasamy CN; Jeyadevan B; Perales-Perez O; Shinoda K; Tohji K; Kasuya A. *Nanotech*, **2003,** *3,* 134–136.

(16) Zheng, H.; Wang, J.; Lofland, S. E.; Ma, Z.; Mohaddes-Ardabili, L.; Zhao, T.; Salamanca-Riba, L.; Shinde, S. R.; Ogale, S. B.; Bai, F.; Viehland, D.; Jia, Y.; Schlom, D. G.; Wuttig, M.; Roytburd, A.; Ramesh, R. *Science*, **2004,** *303,* 661–663.

(17) Pan, Z.; Donthu, S. K.; Wu, N.; Li, S.; Dravid, V. P. *Small* **2006,** *2.2,* 274–280.

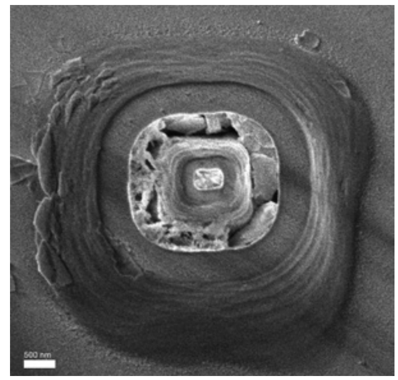

Figure 5. SEM image of the FPN tip with barium titanate in the microchannel.